Proceedings of 8th IOE Graduate Conference
Peer Reviewed
ISSN: 2350-8914 (Online), 2350-8906 (Print)
Year: 2020 Month: June Volume: 8

Flow analysis in eccentric bucket of Micro Pelton turbine: Multiphase modeling with transient state condition

Sourav Dhungana [a], Tri Ratna Bajracharya [b]

[a, b] *Department of Mechanical Engineering, Pulchowk Campus, IOE, TU, Nepal*
Corresponding Email: [a] saurabhdhungana@gmail.com

Abstract
This paper focuses on the flow analysis of eccentric micro Pelton bucket. Mathematical model have been developed to find the torque generated by eccentric bucket about three global axes. Torque has been obtained by calculating unbalanced forces in whirl and flow direction and compared with non-eccentric bucket condition to find the deviation. Numerical simulation has been carried out to study the flow pattern in eccentric bucket and compared to that of non-eccentric bucket at five different angular positions showing velocity contour around the flow. Multiphase analysis at transient state condition has been conducted with complete $140°$ bucket rotation. Torque has been monitored for single bucket and duplicated by using MATLAB software to obtain total torque generated. Maximum Pressure exerted on bucket has been obtained from numerical simulation. The accuracy of the results were conformed by comparison of mathematical and numerical outputs.

Keywords
Pelton Turbine, Flow Analysis, Pelton Bucket Eccentricity, Pelton Multiphase, Pelton Transient

1. Introduction

1.1 Background

Since 1911, a century has been passed, Nepal has been producing electricity from power generation stations under government and private owned companies [1]. Francis and Pelton turbine are preferred in Nepal due to varied altitude ranging from mid hills to high hills. Pelton wheel, a tangential flow impulse turbine, among the various impulse turbines that have been designed and utilized, is considered as the important one [2]. There had been until the end of the last century a noticeable lack of fundamental explanations to the complex hydromechanics of this type of turbines[3].

More focused on distributed generation, nowadays, Micro Hydro Power has been used in huge number across the world due to small investment required and easy to maintain. Micro-hydro-electric project is an efficient and a reliable generator of clean source of renewable energy and uses run-of-river, because it is small in size and only requires very little or no reservoir in order to power the turbine. The water runs straight through the turbine and back into the river or stream to use it for the other purposes with extremely minimal environmental impact on the local ecosystem. Micro-hydro power plants are considered as an attractive option for generating electricity in off grid areas of the country [4]. In impulse turbines water coming out of the nozzle at the end of the penstock is made to strike a series of buckets fitted on the periphery of the wheel [5].

The components to be given most attention in Pelton turbine are nozzle and buckets. The buckets can be replaced easily if its profile is more distorted in the case of bolted buckets used by the small-scale Pelton hydropower [6]. The buckets are shaped in such a way that the ridge in the middle divides the jet into two equal parts which are reversed by almost $180°$ By the reversal almost all the kinetic energy is transferred into force of impulse at the outer diameter of the wheel. Because of the symmetry of the flow almost no axial force is created at the wheel [7]. Whenever the jet is coherent and at the correct speed, the problem could be with the wheel. The mostly likely problem is that the jet is not be hitting the wheel in the correct place which leads to sharp decrease in power as the jet moves outwards. It has been seen that this may lead to noise and vibration [8]. This research is mainly focused on the effect created due to such problem.

In micro Pelton the center wheel is manufactured and

buckets are assembled with the help of nuts and bolts. On the process of assembling bucket, the planar alignment of splitter center line is not conformed due to mechanical processes applied. The splitter with wrong design and not well centered cannot break the jet into equal halves and thus reduces the efficiency. Moreover, to decrease in efficiency, the physical difficulties such as vibration due to force unbalance and uneven erosion on both side of splitter occurs frequently due to uneven pressure and force distribution.

Researches have been conducted on the flow analysis showing that three buckets are sufficient to analyze the power generated by the Pelton wheel [9]. It is also found that the calculation involved in finding power using rpm and torque generated from the numerical simulation can be compared to installed capacity to find out the efficiency of the micro class turbine wheel [10]. Previously studies have shown the comparison of bucket load with specific speed. The variation of bucket loads was plotted with varying specific speeds of the Pelton wheel [11]. A study have been carried out presenting the effect of head and bucket splitter angle on the power output of a Pelton turbine [12]. Previously researches have been conducted on flow analysis of non eccentric bucket but lacks the effect of bucket eccentricity. This study is focused on the flow analysis of eccentric bucket of a micro Pelton turbine.

2. Mathematical Modeling

Whenever the jet interacts with bucket it gets split into two equal halves. The force exerted by two halves in whirl directions are added to get greater effect whereas the force exerted by two halves in flow direction are cancelled out as they are opposite to each other in direction. The summary of specification of test rig used for this study is presented in Table 1.

Table 1: Plant specifications

Installed Capacity (kW)	2
Speed (rpm)	1500
Pitch Circle Diameter (mm)	175
Net Head (m)	47.719
Discharge (m3/s)	5.345 × 10-3

When the bucket gets eccentric, splitter is unable to divide jet into two equal halves and force exerted in flow direction comes into act, which causes angular alignment of jet velocity at inlet with bucket peripheral velocity. This leads to generation of torque in perpendicular to whirl direction. Equations have been developed for torque generated in perpendicular to whirl direction.

A circular cross section of water jet with radius 'r', center 'C' and jet area 'a' as shown in Figure 1. OC represents the pitch circle radius and is denoted by 'R'. The non-eccentric splitter is represented along Z-axis OZ and when in long run the bucket is displaced by a small angle δ the new position of rotated splitter is represented along PQ. The center of the splitter is displaced by distance x which is represented by CR and the jet is split into two unequal areas, PQRP-the smaller one and $PP1ZQ_1QRP$-the larger one. The force is assumed to act on the geometric centroid of split area of jet, T for smaller area and S for larger area.

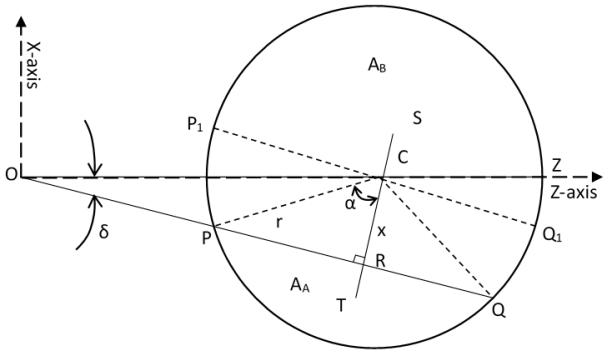

Figure 1: Cross section of water jet showing eccentric splitter

The displacement of splitter measured perpendicularly from center of jet is given by,

$$x = R \times \ sin\delta$$

The angle α can be calculated as,

$$\alpha = \cos^{-1}\left(\frac{x}{r}\right)$$

The area covered by area A is given by,

$$Area\ (A_A) = \frac{r^2}{2}\left(2\alpha - \sin\left(2\alpha\right)\right)$$

The centroid of the area A measured from the splitter center is,

$$\bar{x}_A = \frac{2r^3 sin^3\alpha}{3A_A} - x$$

Whirl velocity (v_{win}), flow velocity ($v_{f\,in}$), relative velocity (v_{rin}) and angle between between inlet jet and peripheral wheel velocity (ψ) at inlet is given by,

$$v_{win} = vcos\psi$$

$$v_{f_{in}} = v sin\psi$$

$$v_{rin} = \sqrt{(V_{win} - u)^2 - V_{f_{in}}^2}$$

The velocity triangle at the inlet and outlet of the area A is shown in Figure 2.

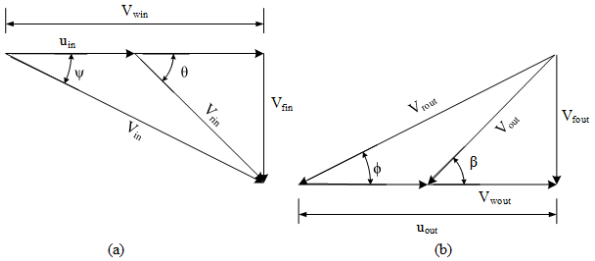

Figure 2: Velocity triangle at (a) Inlet and (b) Outlet of Area A

Whirl velocity (v_{wout}), flow velocity ($v_{f_{out}}$) and relative velocity (v_{rout}) between outlet jet and peripheral wheel velocity at outlet is given by,

$$v_{wout} = v_{rout} cos\phi$$

$$v_{f_{out}} = v_{rout} sin\phi$$

$$v_{rout} = v_{rin}$$

The force exerted to the bucket by the jet in the whirl direction is given by,

$$F_{A_w} = \rho A_A v (v_{win} + v_{wout})$$

Similarly, force exerted to the bucket by the jet in the flow direction is given by,

$$F_{Af} = \rho A_A v \left(v_{f_{out}} + v_{f_{in}}\right)$$

The area covered by the area B is given by,

$$Area\ (A_B) = \frac{r^2}{2}(2\pi - 2\alpha + \sin(2\alpha))$$

The centroid of the area B measured from the splitter centroid is,

$$\bar{x}_B = \frac{2r^3 sin^3\alpha}{3A_B} + x$$

Whirl velocity (v_{win}), flow velocity ($v_{f_{in}}$) and relative velocity (v_{rin}) between inlet jet and peripheral wheel velocity at inlet and whirl velocity (v_{wout}), flow velocity ($v_{f_{out}}$) and relative velocity (v_{rout}) between outlet jet and peripheral wheel velocity at outlet of Area B is calculated as similar to Area A. The velocity triangle at the inlet and outlet of the area B is shown in Figure 3.

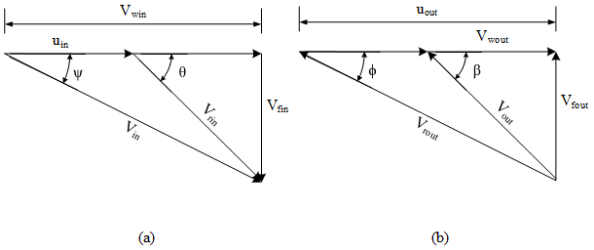

Figure 3: Velocity triangle at (a) Inlet and (b) Outlet of Area B

So, force exerted to the bucket by jet in the whirl direction is given by,

$$F_{B_w} = \rho A_B v (v_{win} + v_{wout})$$

Similarly, force exerted to the bucket by jet in flow direction is given by,

$$F_{Bf} = \rho A_B v \left(v_{f_{out}} - v_{f_{in}}\right)$$

Now, using forces in whirl and flow directions in Area A and B, torque about three axes are calculated. The torque about X-axis is given by,

$$\tau_{xshaft} = (F_{Aw} + F_{Bw}) \times R \times \eta_h \times \eta_m \times \eta_v$$

Similarly, torque about Y-axis is given by,

$$\therefore \tau_{y_{shaft}} = \left(F_{Bf} - F_{A_f}\right) \times R \times \eta_h \times \eta_m \times \eta_v$$

Torque about eccentric splitter is calculated as,

$$\tau = F_{Bw} \times \bar{x}_B - F_{A_w} \times \bar{x}_A$$

Using torque about splitter, the torque about Z-axis is given by,

$$\tau_Z = \tau\, Cos\delta$$

The summary of torques about three axes with two different cases: normal and 1°eccentric bucket is shown in Table 2.

Table 2: Torque about X, Y and Z-axis with varied eccentric angle

Eccentricity (δ)	Torque (Nm)		
	X-axis	Y-axis	Z-axis
0°	12.673	0	0
1°	12.672	-0.206	0.257

3. Flow Analysis

The steps involved in numerical simulation is shown in Figure 4.

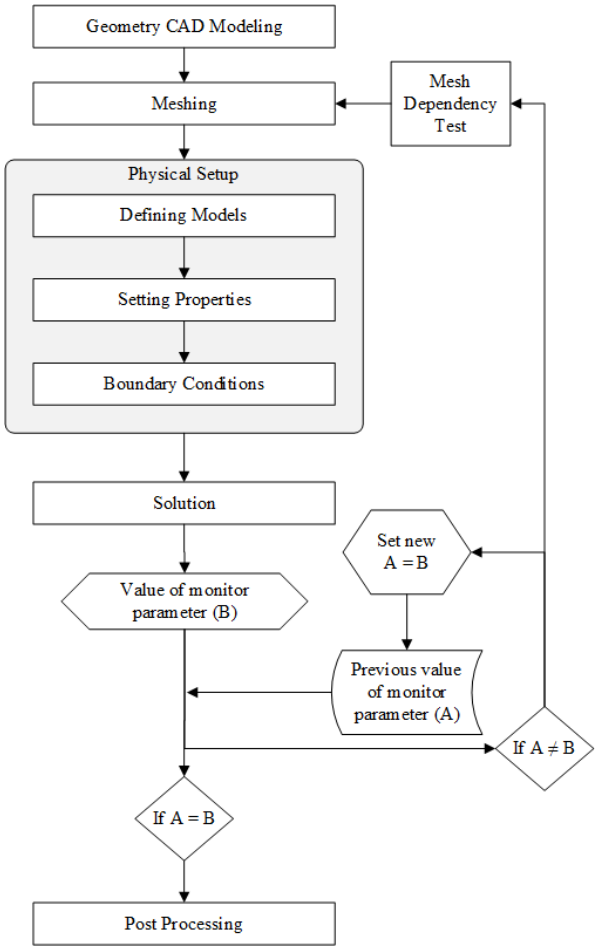

Figure 4: Steps in a computational analysis

3.1 CAD modelling of Fluid Domain

The fluid domain was designed using the ANSYS CAD modelling application, DesignModeler. The geometries consisting the fluid domain was quite simple so the DesignModeler was used. The bucket designed in CATIA P3 V5-6 R2017 was imported to DesignModeler and Boolean function was used to remove the imported bucket region. Figure 5 shows complete CAD drawing of bucket used for the analysis.

Rotating and stationary domain were modelled separately. The stationary domain consists of water jet and a thin layer of air surrounding rotating domain and rotating domain consists of the region around the buckets where water flows excluding the bucket reqion. The rotating domain rotates and the stationary domain remains fixed during the simulation. Both domains are 140 degrees extended to obtain the complete torque curve.

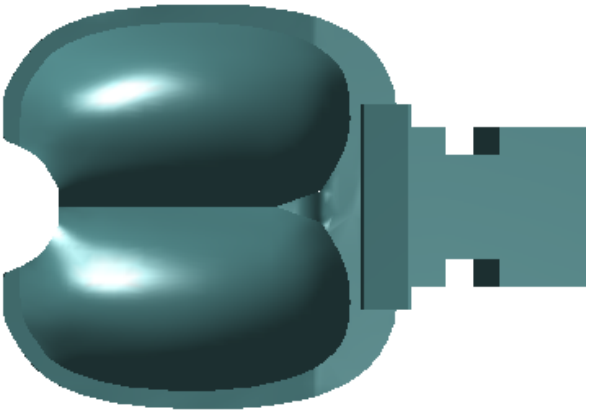

Figure 5: CAD of bucket used

3.2 Meshing

Two standalone meshing components were created for stationary and rotating domain in the ANSYS workbench to mesh both domains separately. The rotating domain shown in Figure 6 consists of complex geometries so it was meshed separately using “advanced size function” turned on. The body sizing with “Body of Influence” was used to cover the water jet region with fine mesh when interacting with all three buckets. Similarly, other two body sizing with “Body of Influence” were used at the water outlet from the bucket with fine mesh to capture the back flow of water. Since the more focus is given to the middle bucket flow the “Face Sizing” with “Inflation” consisting of smaller elements was used in the front face to capture the boundary flow at the bucket.

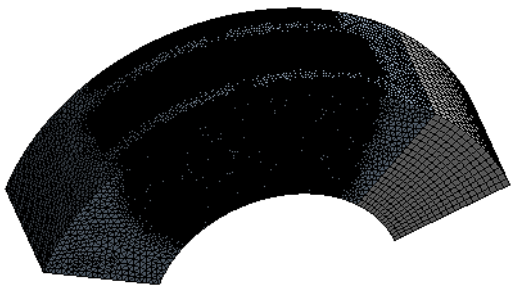

Figure 6: Meshing of Rotating Domain

In the stationary domain the jet region was fine meshed with inflation layer used at the jet wall region to capture the boundary flow in near the jet wall and interaction between air-water interface as shown in Figure 7.

Figure 7: Meshing of Stationary Domain

3.3 Computational Physics Setup

A standalone CFX component was created in ANSYS workbench and the meshes from two components namely, rotating and stationary mesh were transferred to "Setup" component. CFX-Pre consists of various tabs which defines all parameters to be considered while conducting the simulation.

Analysis Type

The transient option with adaptive time steps was chosen. With adaptive time steps and the option "Num. Coeff. Loops" chosen, the solver automatically adjusts the time step size based on the number of coefficient loops used in solving the current time step. The time duration option was set to "Total Time" with the expression "TotalTime". This expression equals the time it takes for the rotating domain to rotate 140 degrees.

Domains

Two domains were created, one for stationary and one for rotating part. The domain type was selected as "Fluid Domain" with coordinate frame selected with origin at center of the wheel. Two fluids, Air and Water were defined with continuous fluid morphology because fluids form continuous connected region throughout the simulation. The reference pressure was set to 1 atm. "Buoyancy Model" was set as "Buoyant" option to provide the effect of gravity in positive Z-axis direction. The "Buoyancy Reference Density" was set to 1000 kg/m3, which is approximate density difference between Water and Air. The flow was multiphase consisting the water and air fluids with homogeneous model because both the phases share the flow field, velocity field, turbulence field and so on near the interface boundary. The "Standard Free Surface Model" was used because the fluid phases are distinct at the interface. Heat transfer mode was set to none to neglect the heat transfer during the simulation. "Surface Tension Coefficient" was set to 0.7 N/m in the "Fluid Pair Models" tab to capture the nature of interaction between water and air in this multiphase conditions. The primary fluid was set to water with continuum surface force surface tension model. Since the analysis is transient in nature the initial conditions are set. Each cartesian velocity components were set to zero with relative static pressure of 0 Pa. Initial volume fraction for air and water was set to 1 and 0 respectively assuming that the domains are fully covered by air at the initial phase. To provide the rotation to rotating domain, "Domain Motion" was set to Rotating with the Angular Velocity equal to expression "AngVel". The rotation was provided along positive X-axis. For the stationary domain, Domain Motion was set to stationary.

Boundary Conditons

While defining the boundary conditions a naming with abbreviations was followed to maintain the short boundary names. Each three buckets is named as Top (T), Middle (M) and Bottom (B) with two boundary names. Middle bucket consists of two boundaries namely, MB for the main flow region and MBC for the complete middle bucket surface. Similarly, TB, TBC for top bucket and BB, BBC for bottom bucket were defined. The buckets were defined as smooth wall with no slip conditions. When water enters the rotating domain the air is pushed out of the rotating domain through the openings named as "RotOpen" set to as "Opening" to entertain the flow of air in and out. The initial volume fraction of air at "RotOpen" was set to 1 with relative pressure of 0 Pa. Similar values were defined for the "StatOpen" which corresponds the opening boundary at stationary domain. The "JetWall" boundary was defined as a wall with no slip conditions and smooth wall. This appears as a wall covering the jet and air surrounding the jet. The interaction between the jet and air can be captured. "JetInlet" was defined as an inlet with the normal inlet velocity set to the expression "InletVel" normal to the "JetInlet" boundary. In the initial condition the theoretical inlet velocity and angular velocity was used to simplify the nature of simulation. The initial volume fraction of air and water was set to 0 and 1 respectively. "StatInlet" was defined as the inlet for the air flow with very small initial velocity. The volume fraction of air and water was set to 1 and 0 respectively.

Solver Control and Output Control

The main required output is the total torque on the middle bucket which was monitored thoroughly during simulation. A monitor for the expression "TorqueMBC", "TorqueMBCy" and TorqueMBCz" was set to capture the torque in middle bucket in each three axis x, y and z respectively saving output results in each timestep which makes the torque curves more smooth.

3.4 Solution using CFX-Solver Manager

The solution was obtained conducting the simulations by CFX-Solver Manager until the residual target was met. An overview of the setup used in all simulations is presented in the Table 3.

Table 3: Overview of the basic setup for simulations

Solver	ANSYS CFX 19.0
Time Discretization	Transient
Advection Scheme	High Resolution
Transient Scheme	Second Order Backward Euler
Turbulence Model	SST with automatic wall function
Multiphase Model	Homogeneous model: Standard Free Surface Model
Surface Tension Model	Continuum Surface Force: Primary fluid as water
Convergence Criteria	RMS with Residual Target of 1.15×10^{-5}
Hardware	Processor: Intel i5-8400 @ 2.81 GHz 6 Cores Memory: 16 GB

3.5 Post Processing

The torque form simulation was obtained at the middle bucket only so the post processing was required to duplicate the obtained torque and obtain total torque. The changing timestep size due to adaptive timesteps made the problem quite complicated so MATLAB coding was preferred instead of Excel table operation. The bucket frequency was calculated as $f_Z = \frac{\omega Z}{2\pi}$ which gave the time period of single bucket as $t = \frac{1}{f_z}$. To find the total torque, torque from single bucket was duplicated 'n' times and each torque curves were shifted by $n \times \frac{1}{fz}$ seconds. This gives a steady state reading of the torque in a certain portion.

The result from numerical simulation is compared with the mathematical output and seems to be in agreement. Figure 8 showa the torque generated by non-eccentric bucket about X-axis.

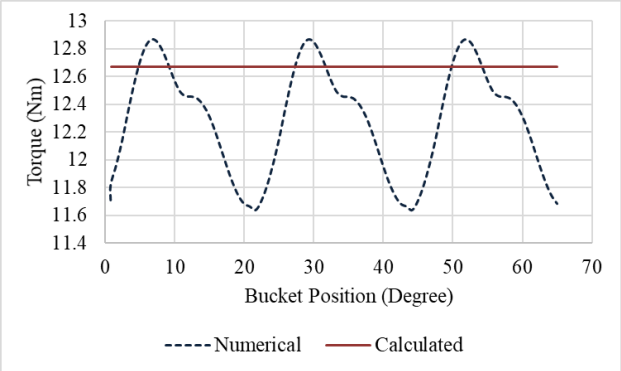

Figure 8: Torque about X-axis with no eccentricity

Figure 9 shows torque generated by eccentric bucket about X-axis. It can be seen that the torque is reduced as compared to Fiugre 8.

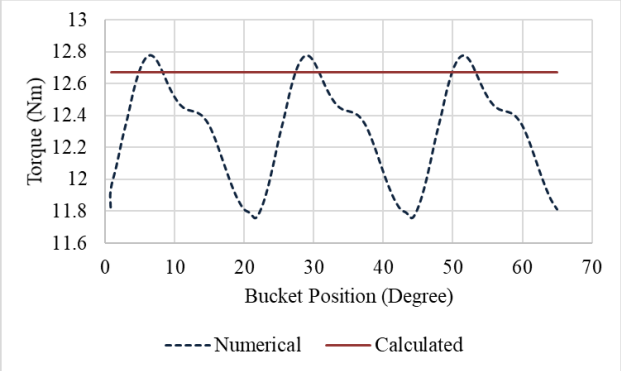

Figure 9: Torque about X-axis with 1° eccentricity

Figure 10 shows the torque generated by eccentric bucket about Y-axis due to unequal forces in flow direction in eccentric bucket.

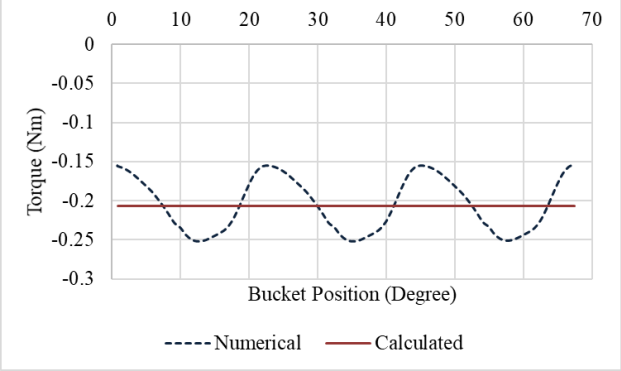

Figure 10: Torque about Y-axis with 1° eccentricity

Figure 11 shows the torque generated by eccentric bucket about Z-axis due to unequal forces on two sides of splitter in whirl direction.

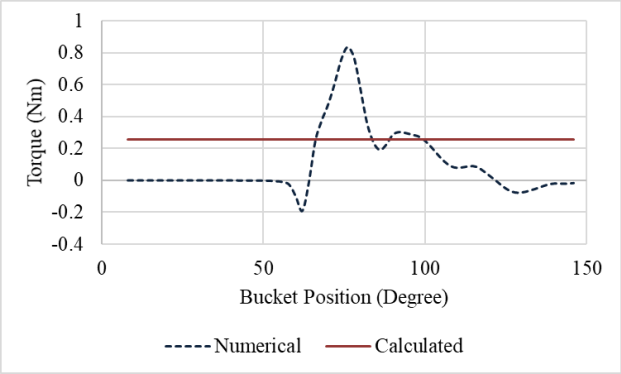

Figure 11: Torque about Z-axis with 1° eccentricity

Figure 12 shows the pressure contour at normal and eccentric buckets at same timestep. It can be seen that more pressure is localised at one side of splitter in eccentric bucket whereas, the normal bucket has equally distributed pressure on both sides of splitter with maximum presseure of 108 kPa and 135 kPa respectively at perpendicular angular position to water jet.

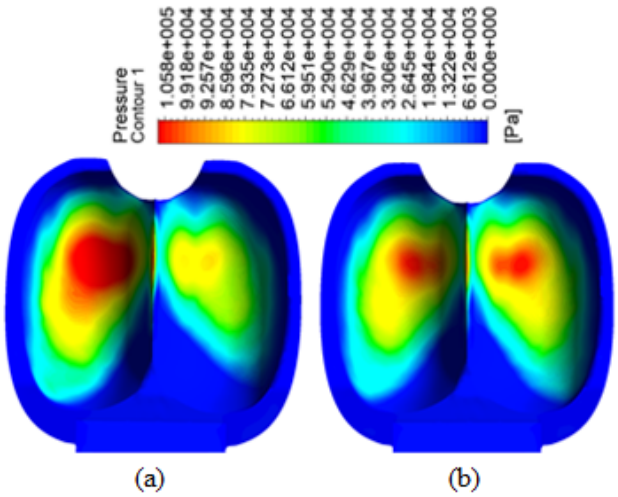

Figure 12: Pressure contour at (a) 1° eccentric bucket (b) Normal condition

Figure 13 shows the flow comparison on normal and 1° eccentric bucket at five different angular positions. The colour represents the velocity of water at that frame. One side of bucket is bearing more load of water causing the generation of unbalanced torques, displaying water volume fraction above 0.7. Angular position 88° to 100° shows middle bucket bearing more back-splash in eccentric bucket on one side.

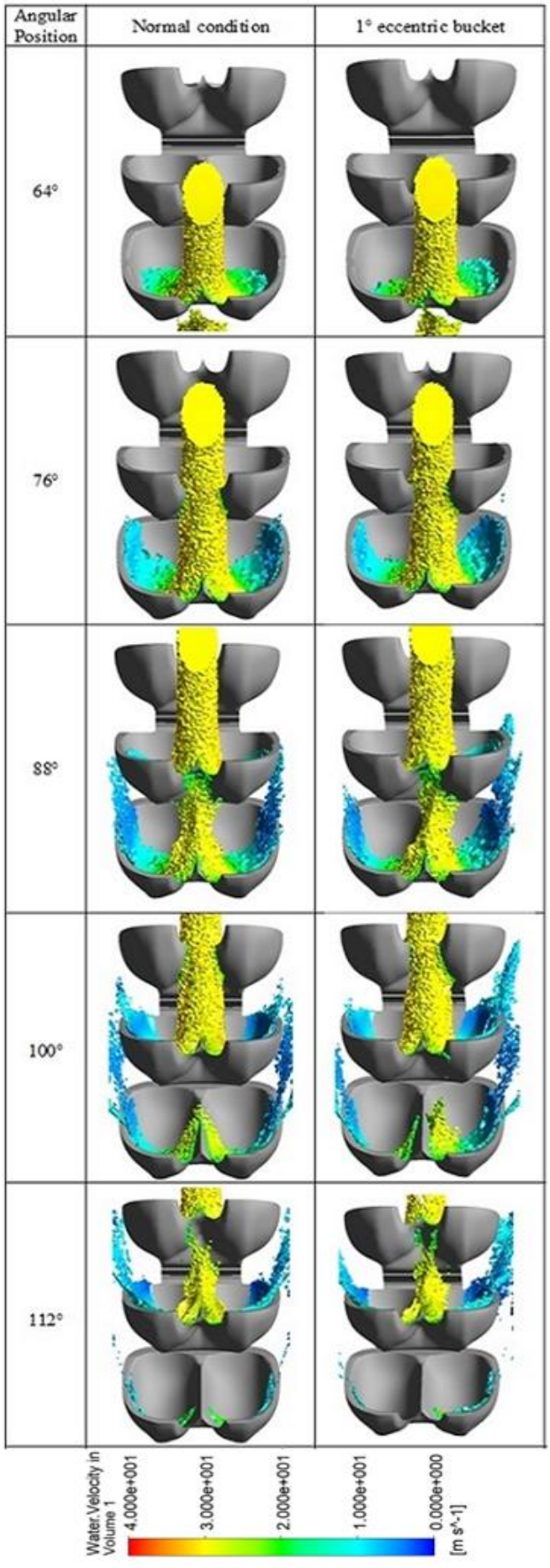

Figure 13: Flow comparison between non-eccentric and 1° eccentric bucket (Colour represents velocity of water with volume fraction above 0.7)

Figure 14 shows the error expressed in percentage between mathematical and numerical simulation results of torque generated by eccentric bucket about three global axis when perpendicular to water jet. All three errors are found to be less than 1.5% which validates the results obtained from numerical simulation. The absolute value of torque is presented.

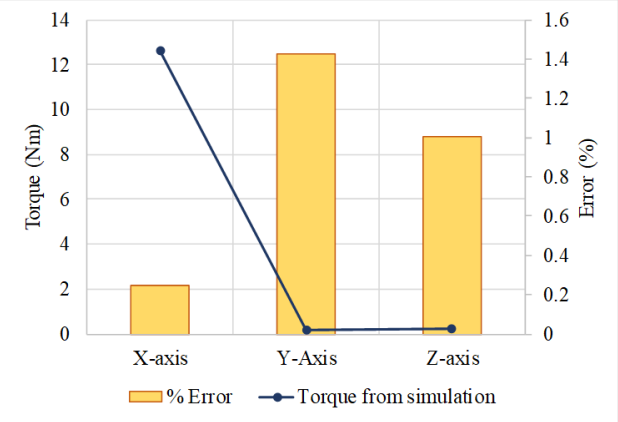

Figure 14: Torque calculated by numerical simulation for 1° eccentric bucket and its error with calculated value

4. Conclusion

A mathematical model is developed to find the torque generated by eccentric bucket about three global axis. The torque about X-, Y- and Z-axis were found to be 12.672 Nm, -0.206 Nm and 0.257 Nm respectively. Flow analysis is performed in ANSYS and simulated numerically. From flow analysis torque was monitored and plotted against mathematical results. Flow pattern on normal and eccentric bucket was studied and compared. The difference in maximum pressure exerted to bucket was found to be 27 kPa in normal and eccentric condition obtained from pressure contour.

Future Enhancements

The research work can be further carried out by conducting structural and fatigue analysis. It is a new approach of conducting flow analysis of eccentric Pelton bucket. So, vibration analysis can also be done to know the performance and reliability of turbine.

Acknowledgments

The authors would like to acknowledge Institute of Engineering [IOE] and Department of Mechanical Engineering, Pulchowk Campus for their support and opportunity.

References

[1] NEA. Nepal electricity authority, generation directorate. Annual report, Nepal Electricity Authority, Kathmandu, Nepal, 2019.

[2] RK Rajput. *Fluid Mechanics and Hydraulic Machines*. by S. Chand Publication, 1998.

[3] Zhengji Zhang. *Pelton turbines*. Springer, 2016.

[4] Loice Gudukeya and Ignatio Madanhire. Efficiency improvement of pelton wheel and crossflow turbines in micro-hydro power plants: case study. *Int J Eng Comput Sci*, 2(2):416–432, 2013.

[5] Bilal Abdullah Nasir et al. Design of micro-hydro-electric power station. *International Journal of Engineering and Advanced Technology*, 2(5):39–47, 2013.

[6] Rainbow Micro Hydro. *Rainbow Micro Hydro Instruction Manual*. Rainbow Power Company Limited, 2001.

[7] Markus Eisenring. *Micro pelton turbines*. SKAT, 1991.

[8] Jeremy Thake. The micro-hydro pelton turbine manual: Design, manufacture and installation for small-scale hydropower. Technical report, ITDG publishing, 2000.

[9] Amod Panthee, Hari Prasad Neopane, and Bhola Thapa. Cfd analysis of pelton runner. *International Journal of Scientific and Research Publications*, 4(8):1–6, 2014.

[10] Tuvshintugs Batbeleg and Young-Ho Lee. Numerical prediction of the performance of a micro class pelton turbine. In *IOP Conference Series: Earth and Environmental Science*, volume 163, page 012058. IOP Publishing, 2018.

[11] Bjørn W Solemslie and Ole G Dahlhaug. Studying the effects of jet alignment in pelton units. *Int. J. Hydropower Dams*, 22(3):78–83, 2015.

[12] Chukweneke Jeremiah. Analysis and simulation on effect of head and bucket splitter angle on the power output of a. *International Journal of Engineering*, 5(03):8269, 2014.